a. Title

Primary 12α-hydroxylated bile acids lower hepatic iron concentration in rats

b. Author names

Shota Hori, [1] Minako Satake, [1] Ohji Kohmoto, [1] Ryo Takagi, [2] Kazufumi Okada, [2] Satoru Fukiya, [1] Atsushi Yokota, [1] Satoshi Ishizuka [1]

c. Author affiliations

[1] Division of Fundamental Agriscience Research, Research Faculty of Agriculture, Hokkaido University, Sapporo, 060-8589, Japan.

[2] Clinical Research and Medical Innovation Center, Hokkaido University Hospital, Sapporo, 060-8648 Japan.

d. Sources of support

This work was supported by JSPS KAKENHI Grant Numbers 16K14917, 19H2900 and JST COI Grant Number JPMJCE1301

e. Conflict of Interest and Funding Disclosure

No conflicts of interest

f. Corresponding Author

Satoshi Ishizuka, Ph.D.

Laboratory of Nutritional Biochemistry, Research Faculty of Agriculture

Hokkaido University, Sapporo, Hokkaido 060-8589, JAPAN

Tel: +81 11 706 3352, zuka@chem.agr.hokudai.ac.jp

g. The word count for the entire manuscript (introduction through discussion).

4041

h. The number of figures (to print, not Supplementary data).

3

i. The number of tables (to print, not Supplementary data).

0

j. Supplementary data submitted.

Yes

k. A running title of 50 or fewer characters and spaces.

12α-Hydroxylated bile acids and liver iron

l. a list of abbreviations and their definitions for all abbreviations used in the text

12αOH BA, 12α-hydroxylated BA; BA, bile acid; *Bmp6*, bone morphogenetic protein 6; DCA, deoxycholic acid; *Dmt1*, Divalent metal transporter 1; *Fpn*, ferroportin; *Fth1*, ferritin heavy chain 1; HF, high-fat; *Hfe2*, homeostatic Fe regulator 2; *Hamp*, hepcidin antimicrobial peptide; *Hmox1*, heme oxygenase 1; *Hp*, haptoglobin; *Hpx*, hemopexin; Il, interleukin; *Lcn2*, lipocalin 2; LCN2, lipocalin 2, *Lcn2r*, lipocalin 2 receptor; *Rplp0*, ribosomal protein lateral stalk subunit P0; *Tfr1*, transferrin receptor 1; *Tfr2*, transferrin receptor 2; TCA, taurocholic acid; TDCA, taurodeoxycholic acid; TIBC, total iron-binding capacity; UIBC, unsaturated iron-binding capacity; *Zip14*, zrt- and irt-like protein 14

Primary 12α-hydroxylated bile acids lower hepatic iron concentration in rats

Shota Hori, Minako Satake, Ohji Kohmoto, Satoru Fukiya, Atsushi Yokota, Satoshi Ishizuka

Abstract

Background: Primary 12α-hydroxylated bile acids (12αOH BAs) enhance intestinal iron uptake due to their ability *ex vivo* to chelate iron. However, no information is available on their role *in vivo*, especially in the liver.

Objective: We investigated the effect and mechanism of primary 12αOH BAs on hepatic iron concentration *in vivo*.

Methods: Male WKAH/HkmSlc rats aged 4–5 weeks were fed a control diet or one with cholic acid (CA; 0.5 g/kg diet), the primary 12αOH BA, for 2 weeks (Study 1) or 13 weeks (Study 2). In Study 3, rats fed the same diets were given drinking water alone or containing vancomycin (200 mg/L) for 6 weeks. The variables measured included food intake (Studies 1-3), BA profiles (Studies 1 and 3), hepatic iron concentration (Studies 1-3), fecal iron excretion (Studies 1 and 2), iron-related liver gene expression (Studies 2 and 3), and plasma iron-related factors (Studies 2 and 3).

Results: In Study 1, CA feed reduced the hepatic iron concentration (-16%; $P = 0.005$) without changing food intake and fecal iron excretion. In Study 2, we found a significant increase in the

aortic plasma concentration of lipocalin 2 (LCN2*;* +65%; $P < 0.001$), an iron-trafficking protein. In Study 3, we observed no effect of vancomycin treatment on the CA-induced reduction of hepatic iron concentration (-32%; $P < 0.001$) accompanied by increased plasma LCN2 concentration (+72%; $P = 0.003$) in the CA-fed rats despite a drastic reduction in secondary 12αOH BA concentration (-94%; $P < 0.001$) in the aortic plasma.

Conclusions: Primary 12αOH BAs reduced the hepatic iron concentration in rats. LCN2 may be responsible for the hepatic iron lowering effect of primary 12αOH BAs by transporting iron out of the liver.

Keywords: 12α-hydroxylated bile acid; high-fat diet; iron deficiency; lipocalin 2; primary bile acid

Introduction

Essential trace elements are required to maintain proper physiological functions in the body (1). Excess and deficiency of trace elements causes malfunctions (2). Alterations in the distribution of essential trace elements have been observed in several metabolic disorders, such as obesity, diabetes, nonalcoholic fatty liver disease, and cardiovascular disease in humans (3). Although it is

well known that essential trace elements play a crucial role in health and disease (3), few researchers have addressed why such changes occur in the metabolism of trace elements under disease conditions. This appears to be due to limited knowledge about host factors that modulate the *in vivo* metabolism of essential trace elements.

12α-hydroxylated bile acid (12αOH BA), an end product of cholesterol catabolism in the liver, may influence liver iron metabolism. The primary 12αOH BAs in humans are cholic acid (CA). Primary 12αOH BAs are metabolized by gut microbiota to secondary 12αOH BAs mainly via 7α-dehydroxylation during transit through the colon (4). A major secondary 12αOH BA is deoxycholic acid (DCA), which is generated from CA. Notably, we recently found that consumption of a HF diet results in a specific increase in 12αOH BAs, such as taurocholic acid (TCA) and DCA, in bile and feces, respectively (5). A specific increase in 12αOH BAs has also been reported in humans with insulin resistance (6), obesity (7), and high-fat (HF) diet consumption (8). The fasting serum concentrations of CA and DCA in obese humans were 4-fold and 1.5-fold higher than those in non-obese humans, respectively (7). It has been reported that HF diet feeding for 5 to 12 weeks induces hepatic iron accumulation in rats (9–11). Mounting evidence has suggested that iron overload increases the risk of several chronic metabolic diseases, such as type 2 diabetes, obesity, nonalcoholic fatty liver disease, and atherosclerosis (12). Interestingly, e*x vivo*

studies have shown that primary 12αOH BAs, such as TCA, enhance the intestinal uptake of calcium and iron due to their high affinity to bind multivalent cations (13,14). These findings suggest that an increase in 12αOH BAs influences the *in vivo* metabolism of hepatic trace elements, especially iron. However, no information is available on the effect of 12αOH BAs on hepatic trace elements, including iron, *in vivo*.

In the present study, we hypothesized that an increase in primary 12αOH BAs alter hepatic iron concentration in comparison with other trace elements (calcium, copper, chromium, manganese, magnesium, and zinc) by changing fecal iron excretion. We investigated the *in vivo* effect of an increase in primary 12αOH BAs on hepatic iron concentration, food intake, fecal iron excretion, liver iron-related gene expression, and plasma iron-trafficking proteins to explore the underlying regulatory mechanism of primary 12αOH BAs.

Material & Methods

Animal experiments and sample collection

This study was approved by the Institutional Animal Care and Use Committee of the National Corporation Hokkaido University (approval number: 17-0119 and 19-0161), and all animals were maintained following the Hokkaido University Manual for Implementing Animal Experimentation. Wistar King A Hokkaido male rats (WKAH/HkmSlc, 3 weeks old, NBRP Rat No: 0154), an inbred strain originating from Wistar rats that weigh 40–70 g, were purchased from Japan SLC, Inc. (Shizuoka, Japan). Rats were housed individually in a wire-bottomed cage and provided with ad libitum access to food and water. The experiment was performed in a controlled environment at 22 ± 2 ℃ and 55 ± 5% humidity with a 12 h light/dark cycle (08.00 a.m.–08.00 p.m. light period). The rats were fed a control diet based on the AIN-93G formulation (15) (Supplemental Table 1) for an acclimation period (2 weeks in Study 2; 1 week in Study 1 and Study 3). The iron concentration in the diet was 35 mg/kg. The rats were divided into several groups in each experiment to have comparable average body weights based on measurements on the day when the test diet was initiated. Body weight and food intake were measured every two days. All rats were not feed-deprived prior to exsanguination in the experiments. The scheme of the present study is shown in Supplemental Figure 1.

In Study 1, to investigate the impact of an increase in 12αOH BAs on hepatic iron concentration in comparison with other trace elements (calcium, copper, chromium, manganese,

magnesium, and zinc), acclimated male WKAH/HkmSlc rats (4 weeks old and 65–90 g; Japan SLC, Inc.) were fed a control (n = 8) or CA diet (n = 9) (Supplemental Table 1) for 2 weeks. The CA diet, which mimics the BA environment in rats fed a HF diet (5,16), causes an increase in 12αOH BAs such as CA and DCA (17).

In Study 2, we performed a long-term CA feeding experiment to confirm the decrease in liver iron concentration observed in Study 1 and explore factors related to iron reduction in the liver. Acclimated male WKAH/HkmSlc rats (5 weeks old and 100–150 g; Japan SLC, Inc.) were fed a control or CA diet (n = 12 per group) for 13 weeks.

In Study 3, we investigated whether the metabolism of 12αOH BAs by gut microbes influences hepatic iron concentration. Acclimated male WKAH/HkmSlc rats (4 weeks old and 65–90 g; Japan SLC, Inc.) were fed either a control or CA diet treated with or without vancomycin (200 mg/L) (FUJIFILM Wako Pure Chemical Corporation, Osaka, Japan) (n = 8 per group) in drinking water for 6 weeks. At week 4, we confirmed a significant decrease in fecal DCA concentration (data not shown) after vancomycin treatment.

Sample collection

144 At the end of each experiment, the portal and aortic blood were collected under anesthesia
145 with sodium pentobarbital (50 mg/kg body weight) using a syringe containing heparin (final
146 concentration of 50 IU/mL) and aprotinin (final concentration of 500 kilo IU/mL). Plasma was
147 separated by centrifugation at 2,000 × *g* for 10 min at 4 °C. After euthanization by exsanguination,
148 the liver was immediately removed, rinsed with saline, and weighed. Thereafter, the left lateral
149 lobe(18) was used for analysis. Feces were collected during the last two days of the test period
150 (beginning from 10 a.m. for 48 h) and weighed. The collected liver, plasma, and feces were stored
151 at -80°C until analysis. The jejunal contents (upper 10 cm of the small intestine) were collected in
152 Study 1 to measure the BA composition.
153
154 ***Determination of the iron concentration and parameters***
155 Concentrations of trace elements (iron, chromium, manganese, copper, zinc, magnesium,
156 and calcium) in the liver (19) were simultaneously analyzed using a DRC-e inductively coupled
157 plasma mass spectrometer (ELAN; Perkin Elmer, Waltham, MA, USA). The liver is the main iron
158 storage unit in the body, and hepatic iron concentration correlates with total body iron stores (20);
159 thus, we measured hepatic iron concentration as previously described (19). Fecal iron concentration
160 was also measured as described above. The apparent absorption rate was calculated as follows:

Apparent iron absorption rate (%)

= (total iron intake−fecal iron excretion) / total iron intake × 100

To measure ferritin levels in the liver, 20 mg of liver tissue collected from the left lateral lobe (18) was homogenized and sonicated with 500 μL of cold phosphate-buffered saline on ice. After centrifugation at 14,000 × *g* for 10 min, the supernatants were collected and properly diluted to measure ferritin levels using the Ferritin (Rat) ELISA Kit (Abnova, Taipei, Taiwan). The values were normalized to protein levels in the supernatants determined using a TaKaRa BCA Protein Assay Kit (Takara Bio, Shiga, Japan). Plasma iron and blood hemoglobin levels were determined using an Iron Assay Kit LS (Ferrozine method; Metallogenics, Chiba, Japan) and a Hemoglobin Colorimetric Assay Kit (Cayman Chemical, Ann Arbor, Michigan, USA), respectively. Plasma unsaturated iron-binding capacity (UIBC), transferrin concentration, and LCN2 concentration were determined using a microassay UIBC quantification kit (Metallogenics), a Rat Transferrin ELISA Kit (Life Diagnostics, Carlsbad, CA, USA), and a CircuLex Rat NGAL/Lipocalin-2 ELISA Kit (Medical & Biological Laboratories Co., Ltd., Aichi, Japan), respectively. The total iron-binding capacity (TIBC) was determined as the sum of the plasma iron and UIBC.

BA analysis

BAs in several tissues and plasma were extracted (21,22) and analyzed (23) as previously described. The primary 12αOH BAs measured were as follows: 5β-cholanic acid-3α,7α,12α-triol (CA); 5β-cholanic acid-3α,7α,12α-triol-*N*-(2-sulphoethyl)-amide (TCA); and 5β-cholanic acid-3α,7α,12α-triol-*N*-(carboxymethyl)-amide (glycocholic acid, GCA). The primary non-12αOH BAs measured were as follows: 5β-cholanic acid-3α,7α-diol (chenodeoxycholic acid, CDCA); 5β-cholanic acid-3α,7α-diol-*N*-(2-sulphoethyl)-amide (taurochenodeoxycholic acid, TCDCA); 5β-cholanic acid-3α,7α-di-ol-*N*-(carboxymethyl)-amide (glycochenodeoxycholic acid, GCDCA); 5β-cholanic acid-3α,6β,7α-triol (α-muricholic acid, αMCA); 5β-cholanic acid-3α,6β,7β-triol (β-muricholic acid, βMCA); 5β-cholanic acid-3α,6β,7α-triol-*N*-(2-sulphoethyl)-amide (tauro-α-muricholic acid, TαMCA); and 5β-cholanic acid-3α,6β,7β-triol-*N*-(2-sulphoethyl)-amide (tauro-β-muricholic acid, TβMCA). The secondary 12αOH BAs measured were as follows: 5β-cholanic acid-3α,12α-diol (DCA); 5β-cholanic acid-3α,12α-diol-*N*-(2-sulphoethyl)-amide (taurodeoxycholic acid, TDCA); 5β-cholanic acid-3α,12α-diol-*N*-(carboxymethyl)-amide (glycodeoxycholic acid, GDCA); 5β-cholanic acid-3α,12α-diol-7-one (7-oxodeoxycholic acid, 7oDCA); 5β-cholanic acid-3α-ol-12-one (12-oxo-lithocholic acid, 12oLCA); 5β-cholanic acid-12α-ol-3-one (3o12α); and 5β-cholanic acid-3α,7β,12α-triol (ursocholic acid, UCA). The secondary non-12αOH BAs measured

were as follows: 5β-cholanic acid-3α-ol (lithocholic acid, LCA); 5β-cholanic acid-3α-ol-*N*-(2-sulphoethyl)-amide (taurolithocholic acid, TLCA); 5β-cholanic acid-3α-ol-*N*-(carboxymethyl)-amide (glycolithocholic acid, GLCA); 5β-cholanic acid-3α,6α,7β-triol (ω-muricholic acid, ωMCA); 5β-cholanic acid-3α,6α,7β-triol-*N*-(2-sulphoethyl)-amide (tauro-ω-muricholic acid, TωMCA); 5β-cholanic acid-3α,6α,7α-triol (hyocholic acid, HCA); 5β-cholanic acid-3α,6α-diol (hyodeoxycholic acid, HDCA); 5β-cholanic acid-3α,6α-diol-*N*-(2-sulphoethyl)-amide (taurohyodeoxycholic acid, THDCA); 5β-cholanic acid-3α,6α-diol-*N*-(carboxymethyl)-amide (glycohyodeoxycholic acid, GHDCA); 5β-cholanic acid-3α,7β-diol (ursodeoxycholic acid, UDCA); 5β-cholanic acid-3α,7β-diol-*N*-(2-sulphoethyl)-amide (tauroursodeoxycholic acid, TUDCA); 5β-cholanic acid-3α,7β-diol-*N*-(carboxymethyl)-amide (glycoursodeoxycholic acid, GUDCA); and 5β-cholanic acid-3α-ol-7-one (7-oxo-lithocholic acid, 7oLCA).

Quantitative real-time polymerase chain reaction analysis

Liver mRNA expression was measured using TaqMan probes or the SYBR Green method as previously described (19). The TaqMan Gene Expression probes were as follows (Thermo Fisher Scientific Inc., Waltham, MA, USA): Rn00432095_m1 for bone morphogenetic protein 6 (*Bmp6*), Rn00591187_m1 for ferroportin 1 (*Fpn*), Rn00820640_g1 for ferritin heavy chain 1 (*Fth1*),

Rn00584987_m1 for hepcidin antimicrobial peptide (*Hamp*), Rn01265685_g1 for homeostatic Fe regulator 2 (*Hfe2*), Rn00561387_m1 for heme oxygenase 1 (*Hmox1*), Rn00561393_m1 for haptoglobin (*Hp*), Rn00584069_m1 for hemopexin (*Hpx*), Rn03302271_gH for ribosomal protein lateral stalk subunit P0 (*Rplp0*), Rn01474701_m1 for transferrin receptor 1 (*Tfr1*), and Rn01468336_m1 for zrt- and irt-like protein 14 (*Zip14*). The SYBR Green method was performed with specific primer pairs for divalent metal transporter 1 *(Dmt1*, forward: 5′-GAGCCTACAGCTCCCCTTTG-3′, reverse: 5′-CCACCACATACAGTGCCACA-3′; 10 μmol/L), lipocalin-2 (*Lcn2*, forward: 5′-ACTTCCATCCTCGTCAGGGG-3′, reverse: 5′-TCCGTACAGGGTGACTTTGAA-3′; 10 μmol/L), lipocalin 2 receptor (*Lcn2r*, forward: 5′-GCACGGTGGCTGATAGTGAA-3′, reverse: 5′-GTAGTTGAGGAGGGAGGCGA-3′; 10 μmol/L), *Rplp0* (forward: 5′-GGCAAGAACACCATGATGCG-3′, reverse: 5′-GTGATGCCCAAAGCTTGGAA-3′; 5 μmol/L), and transferrin receptor 2 (*Tfr2*, forward: 5′-TCAGACTCTCCGTATCGCCT-3′, reverse: 5′-AAAAGGTCCGAACCAGCTCC-3′; 10 μmol/L). Relative expression levels were calculated for each sample after normalization to *Rplp0* as a reference gene using the standard curve method.

Statistical analysis

Unless otherwise indicated, values are presented as the mean ± SEM. Statistical analysis was performed using JMP version 14.0 software (SAS Institute Inc., Cary, NC, USA). Statistical significance was set at $P < 0.05$ unless specified otherwise. The values of undetectable parameters were considered to be 0 in the statistical analysis. Before statistical analysis, all the data were evaluated for normality and homogeneity of variance using the Shapiro-Wilk and Brown-Forsythe tests, respectively. In two-group comparisons, such as Study 1 and 2 (Figures 1 and 2), a significant difference in mean values between the two groups was determined using the unpaired Student's *t*-test. In cases of violation of the assumptions of normality or homogeneity of variance, the Mann-Whitney U test or Welch *t*-test was applied, respectively. In Study 3, a two-way analysis of variance (ANOVA; CA and vancomycin) was used to evaluate differences in all parameters (Figure 3). Before ANOVA, some of the data from Study 3, such as aortic plasma total secondary 12αOH BAs, TDCA, and LCN2, were log-transformed ($\log_{10}$) to improve the homogeneity of the variance. If there was an undetectable value in a parameter, all the values in the parameter were added 1 before the log-transformation. The means reported in figures were back-transformed for interpretation. A simple effect analysis was employed when there was a significant interaction (CA × vancomycin). We set $P < 0.0125$ (0.05/4) as significance to control for Type I error rate

across the four simple effects. For liver LCN2 gene expression and plasma LCN2 level, outliers were excluded by the Smirnov-Grubbs test. To determine an adequate sample size to identify significant differences in hepatic iron concentration, we performed a power analysis using G*Power (version 3.1.9.4) based on the experimental design: Student's *t*-test (Study 1 and Study 2) and two-way ANOVA (Study 3). We used an α probability of 0.05 and a power of 0.80, and the effect size was estimated using the results from a preliminary study (unpublished results). The required sample sizes were 6-17 (Study 1 and Study 2) and 5-13 (Study 3) rats per group.

Results

Hepatic mineral levels (Study 1)

We tested the hypothesis that an increase in 12αOH BAs modulates hepatic mineral concentrations, especially iron, *in vivo* by altering fecal iron excretion. The concentration of total 12αOH BAs was significantly increased by CA feeding in the jejunal contents (control: 15 ± 1.7 μmol/g vs. CA: 64 ± 9.1 μmol/g; $P < 0.001$) and portal plasma (control: 19 ± 4.0 μmol/L vs. CA: 143 ± 23 μmol/L; $P < 0.001$). On the other hand, there were no significant differences in total non-12αOH BAs in the jejunal contents (control: 5.9 ± 1.3 μmol/g vs. CA: 9.9 ± 4.2 μmol/g; $P = 0.34$)

and portal plasma (control: 16 ± 2.8 μmol/L vs. CA: 14 ± 1.5 μmol/L; $P = 0.53$) between the groups. Detailed BA profiles are shown in Supplemental Tables 2 and 3. Interestingly, short-term CA feeding reduced both liver iron concentration (-16%; $P = 0.005$) and content (-14%; $P = 0.007$) (Figure 1A and B) with no significant differences in food intake, liver weight, final body weight, and fecal iron excretion (Supplemental Table 4). There were no significant differences in the hepatic total amounts of manganese, copper, zinc, magnesium, and calcium (Figure 1B), although the concentrations of chromium, zinc, and magnesium were significantly reduced in CA-fed rats, suggesting that an increase in 12αOH BAs influences hepatic iron metabolism compared to the other minerals.

Hepatic iron and iron metabolism (Study 2)

To confirm the hepatic iron lowering effect of 12αOH BAs observed in Study 1, we further examined whether long-term CA feeding (13 weeks) reduces liver iron concentration in Study 2. CA feeding for 13 weeks also reduced both hepatic iron concentration (-39%; $P < 0.05$) and content (-15%; $P < 0.05$) (Figure 2A and B). There was no significant reduction in liver ferritin concentration in the CA-fed rats ($P = 0.056$) (Figure 2C). Consistent with Study 1, total food intake

277 over 13 weeks and final body weight were not significantly different between the groups, although
278 liver weight was significantly increased in CA-fed rats (Supplemental Table 5). In addition, no
279 significant differences were observed in daily food intake and fecal iron excretion (Figure 2D and
280 E) as well as apparent iron absorption rate between the control and CA-fed rats (control: 32 ± 6.3%
281 vs. CA: 36 ± 5.9%; $P = 0.70$) at the end of the experiment.

282 To examine whether CA feeding induces systemic iron deficiency and anemia, we
283 measured plasma parameters related to iron. There were no significant differences in aortic
284 hemoglobin or aortic plasma iron, ferritin, transferrin, UIBC, TIBC, or transferrin saturation
285 between the control and CA-fed rats (Figure 2F-L).

286 We next investigated the underlying mechanisms by which 12αOH BAs reduce hepatic iron
287 concentration without changing food intake and apparent iron absorption in rats. It has been
288 previously shown that chronic HF diet consumption is associated with decreased hepatic iron
289 concentration (24–28) and increased serum concentration of LCN2 (29), an iron-trafficking protein
290 that can reduce intracellular iron concentration by transporting iron out of the cell (30). Therefore,
291 we hypothesized that the CA diet increased liver *Lcn2* expression and plasma LCN2 concentration.
292 As expected, we found that the CA diet substantially increased liver *Lcn2* expression (+580%; $P <$

0.001) (Figure 2M) as well as the plasma LCN2 concentration (+65%; $P < 0.001$) (Figure 2N). There were no significant differences in the expressions of other possible genes for reducing the hepatic iron concentration in the liver, such as iron transporters (*Tfr1*, *Tfr2*, *Lcn2r*, *Zip14*, *Dmt1*, and *Fpn*), an iron-regulating hormone (*Hamp*), a heme oxygenase (*Hmox1*), an iron storage protein (*Fth1*), *Hamp*-regulating transcription factors (*Bmp6* and *Hfe2*), a heme transporter (*Hpx*), and a hemoglobin transporter (*Hp*) (Figure 2N).

Secondary 12αOH BAs and hepatic iron (Study 3)

To examine whether secondary 12αOH BAs are involved in hepatic iron reduction by CA feeding, rats fed the same diet as that of Study 1 and 2 were treated with vancomycin to reduce secondary BAs. Food intake and body weight were comparable among the groups (Supplemental Table 6). The CA diet significantly increased the total concentration of 12αOH BAs in the aortic plasma regardless of vancomycin treatment (Figure 3A). The concentration of primary 12αOH BAs was significantly elevated in CA-fed rats (Figure 3B). The combination of CA and vancomycin further increased the concentration of primary 12αOH BAs in the aortic plasma. On the other hand, vancomycin treatment significantly decreased secondary 12αOH BAs in CA-fed rats (Figure 3C).

The major primary 12αOH BAs were TCA and CA (Figure 3D and E). The major secondary 12αOH BAs (Figure 3F and G) were TDCA and DCA. The BA profiles in the aortic plasma and liver are shown in Supplemental Tables 7 and 8. Under these conditions, CA supplementation significantly lowered liver iron concentration and content regardless of vancomycin treatment (Figure 3H-J). Consistent with Study 2, increases in hepatic *Lcn2* expression (Figure 2J) and plasma LCN2 concentration (Figure 3K) were associated with a reduction in hepatic iron concentration by CA feeding.

Discussion

Iron is a cofactor for several enzymes and a major component of the oxygen transporter in the body. Many epidemiological studies have shown that an increase in serum ferritin concentration is associated with the development of metabolic syndrome, glucose intolerance, and type 2 diabetes (12). Paradoxically, obese humans show a decrease in serum ferritin concentration (31) and HF

diet-fed animals have lower hepatic iron concentrations (24–28), suggesting that iron overload and deficiency contribute to some metabolic disorders in a different manner. Indeed, an association between low hepatic iron concentration, insulin resistance (32), and hepatic lipid accumulation (19) has been reported. Furthermore, Siddique et al. (33) reported that obesity, diabetes, and metabolic syndrome were more common among nonalcoholic fatty liver disease patients with iron deficiency. Despite these findings, the host factors that regulate iron metabolism are not fully understood.

The objectives of this study were to determine the impact of an increase in 12αOH BAs on hepatic iron concentration compared to other hepatic trace elements (chromium, manganese, copper, zinc, magnesium, and calcium) and examine the underlying molecular mechanisms responsible for the potential alterations in hepatic iron concentration by 12αOH BAs. The data revealed that an increase in 12αOH BAs especially lowered hepatic iron concentration compared to the other hepatic trace elements regardless of no significant changes in food intake, fecal iron excretion, and body weight of the rats (Figure 1A-B, Supplemental Table 4). The reduction in iron concentration may be specific to the liver because there were no alterations in plasma iron-related factors, such as iron concentration and blood hemoglobin level (Figure 2A-F), by the chronic increase in 12αOH BAs. Interestingly, the increase in plasma LCN2 concentration accompanied by an upregulation of liver *Lcn2* expression was negatively associated with the 12αOH BA-induced

342 reduction in hepatic iron concentration. We also demonstrated that primary 12αOH BAs are
343 responsible for these changes rather than secondary 12αOH BAs.

344 Both the concentration and content of hepatic iron were significantly reduced in short-term
345 (Figure 1A and B) and long-term CA feeding (Figure 2A and B) without changing food intake and
346 apparent iron absorption while the hepatic content of other trace elements (chromium, copper,
347 calcium, manganese, magnesium, and zinc) did not significantly change in short-term CA feeding
348 (Figure 1A and B). Intriguingly, the aortic plasma iron concentration as well as aortic blood
349 hemoglobin level did not significantly decrease even after long-term CA feeding for 13 weeks
350 (Figure 2F and H) while both hepatic iron concentration and content significantly decreased. It is
351 possible that the effect of 12αOH BAs on iron metabolism is specific to the liver because the
352 concentration of 12αOH BAs in enterohepatic circulation, such as the portal vein and liver, is much
353 higher than that in systemic circulation.

354 Primary 12αOH BAs, such as TCA, enhanced intestinal iron uptake due to their chelating
355 effect in *ex vivo* studies (13,14). Although this finding is inconsistent with our *in vivo* observations,
356 the promotion of iron uptake occurred mainly at a pre-micellar concentration of TCA while almost
357 no enhancement of iron uptake took place beyond its critical micelle concentrations (13,14). The

TCA concentration in the small intestine was clearly higher than the critical micellar concentration of TCA (8-12 mM) (34) even in control rats (Supplemental Table 2). Therefore, it is speculated that the increase in TCA concentration by CA feeding does not further enhance *in vivo* iron absorption. Dietary iron absorption may not be closely associated with the liver iron-lowering effect of 12αOH BAs.

The liver secretes LCN2 (35), an iron-trafficking protein that delivers or removes iron from the cell based on certain conditions (36). The iron-loaded form of LCN2 increases intracellular iron concentration, whereas the iron-deficient form decreases intracellular iron levels (30). We found that the CA diet remarkably increased liver *Lcn2* gene expression (Figure 2M). It is important to note that there were no significant differences in the expression levels of other liver genes, such as iron transporters and iron exporters (Figure 2M), implying that LCN2 from the liver is a crucial mediator in reducing hepatic iron concentration in CA-fed rats. Plasma LCN2 concentration was also significantly increased in CA-fed rats in addition to an increase in liver *Lcn2* gene expression. These data in conjunction with previous studies suggest that an increase in 12αOH BAs in enterohepatic circulation specifically reduces hepatic iron concentration by increasing the LCN2 plasma iron-deficient form concentration.

374 The aortic plasma concentration of 12αBAs in CA-fed rats was calculated to be 1.7-fold
375 higher than that in the control rats without vancomycin treatment (Figure 3A). This magnitude is
376 close to that of obese humans with type 2 diabetes compared to healthy subjects (approximately 1.8-
377 fold higher) (6). The CA-induced increase in 12αOH BAs would be relevant for the consideration
378 of such human conditions. Importantly, CA feeding increased not only the concentration of primary
379 but also secondary 12αOH BAs in the aortic plasma (Supplemental Table 3). Vancomycin treatment
380 completely reduced the secondary 12αOH BA concentration without changing the total 12αOH BA
381 concentration in the rat aortic plasma (Figure 3A and C). However, vancomycin treatment did not
382 normalize the reduced hepatic iron concentration accompanied by increases in plasma LCN2
383 concentration and liver *Lcn2* expression in CA-fed rats, suggesting that primary 12αOH BAs are
384 responsible for increasing aortic plasma LCN2 concentration and lowering hepatic iron
385 concentration.

386 CA feeding that mimics the BA environment in rats fed a HF diet (5,17) specifically
387 increased 12αOH BAs (Supplemental Tables 2 and 3). It is interesting to note that HF diet
388 consumption may modulate the direction of hepatic iron storage in a time-dependent manner.
389 Hepatic iron accumulation has been observed in animals fed a HF diet for 5 to 12 weeks (9–11)
390 whereas comparable hepatic iron concentrations were found in animals fed a HF diet for 10 to 12

391 weeks (37,38). Surprisingly, further long-term HF diet consumption (12 weeks, 16 weeks, 18
392 weeks, or 31 weeks) is associated with a lowered hepatic iron concentration (24–28). The precise
393 mechanisms through which HF diet consumption regulates hepatic iron concentration in this
394 direction remain unclear, and further studies are necessary to explain the role of 12αOH BAs in the
395 regulation of liver iron concentration. However, we have previously shown that HF diet feeding for
396 8 weeks increased the concentration of primary 12αOH BAs in the portal plasma (16). In addition,
397 an increase in serum LCN2 has been observed in mice fed a HF diet for 12 weeks (29). The data in
398 the present study demonstrated that primary 12αOH BAs enhance plasma LCN2 concentration,
399 which may lower hepatic iron concentration irrespective of food intake and apparent iron
400 absorption. Thus, our findings may partially explain the reason why long-term HF diet consumption
401 reduces hepatic iron concentration.

402 In conclusion, our results showed that primary 12αOH BAs are host factors that reduce
403 hepatic iron concentration. An increase in the concentration of plasma LCN2 due to upregulation of
404 liver *Lcn2* expression may mediate the hepatic iron lowering effect of primary 12αOH BAs by
405 removing iron from hepatocytes in rats.

406

Acknowledgement

S.H., M.S., O.K., S.F., A.Y., and S.I. designed research; S.H., M.S., O.K., S.F., A.Y., and S.I. conducted research; S.H., M.S., R.T., and K.O. analyzed data or performed statistical analysis; S.H. and S.I. wrote paper; S.I. had primary responsibility for final content; All authors have read and approved the final manuscript.

References

1. Goldhaber SB. Trace element risk assessment: essentiality vs. toxicity. Regul Toxicol Pharmacol 2003;38:232–42.

2. Zoroddu MA, Aaseth J, Crisponi G, Medici S, Peana M, Nurchi VM. The essential metals for humans: a brief overview. J Inorg Biochem 2019;195:120–9.

3. Sigel A, Sigel H, Sigel RKO. Interrelations between essential metal ions and human diseases. Springer 2013: 1-573 p.

4. Ridlon JM, Kang D-J, Hylemon PB. Bile salt biotransformations by human intestinal bacteria. J Lipid Res 2006;47:241–59.

5. Yoshitsugu R, Kikuchi K, Iwaya H, Fujii N, Hori S, Lee DG, Ishizuka S. Alteration of bile acid metabolism by a high-fat diet is associated with plasma transaminase activities and glucose intolerance in rats. J Nutr Sci Vitaminol 2019;65:45–51.

6. Haeusler RA, Astiarraga B, Camastra S, Accili D. Human insulin resistance is associated with increased plasma levels of 12α−hydroxylated bile acids. Diabetes 2013;62:4184–91.

7. Haeusler RA, Camastra S, Nannipieri M, Astiarraga B, Castro-Perez J, Xie D, Wang L, Chakravarthy M, Ferrannini E. Increased bile acid synthesis and impaired bile acid transport in human obesity. J Clin Endocrinol Metab 2016;101:1935–44.

8. Wan Y, Yuan J, Li J, Li H, Zhang J, Tang J, Ni Y, Huang T, Wang F, Zhao F, et al. Unconjugated and secondary bile acid profiles in response to higher-fat, lower-carbohydrate diet and associated with related gut microbiota: A 6-month randomized controlled-feeding trial. Clin Nutr 2020;39:395–404.

9. Ahmed U, Oates PS. Dietary fat level affects tissue iron levels but not the iron regulatory gene HAMP in rats. Nutr Res 2013;33:126–35.

10. Meli R, Mattace Raso G, Irace C, Simeoli R, Di Pascale A, Paciello O, Pagano TB, Calignano A, Colonna A, Santamaria R. High fat diet induces liver steatosis and early dysregulation of iron metabolism in rats. PLoS One 2013;8:e66570.

11. Dongiovanni P, Lanti C, Gatti S, Rametta R, Recalcati S, Maggioni M, Fracanzani AL, Riso P, Cairo G, Fargion S, et al. High fat diet subverts hepatocellular iron uptake determining dysmetabolic iron overload. PLoS One 2015;10:e0116855.

12. Fernández-Real JM, Manco M. Effects of iron overload on chronic metabolic diseases. Lancet Diabetes Endocrinol 2014;2:513–26.

13. Sanyal AJ, Shiffmann ML, Hirsch JI, Moore EW. Premicellar taurocholate enhances ferrous iron uptake from all regions of rat small intestine. Gastroenterology 1991;101:382–9.

14. Sanyal AJ, Hirsch JI, Moore EW. High-affinity binding is essential for enhancement of intestinal Fe^{2+} and Ca^{2+} uptake by bile salts. Gastroenterology 1992;102:1997–2005.

15. Reeves PG, Nielsen FH, Fahey GC Jr. AIN-93 purified diets for laboratory rodents: final report of the American Institute of Nutrition ad hoc writing committee on the reformulation of the AIN-76A rodent diet. J Nutr 1993;123:1939–51.

16. Hori S, Abe T, Lee DG, Fukiya S, Yokota A, Aso N, Shirouchi B, Sato M, Ishizuka S. Association between 12α-hydroxylated bile acids and hepatic steatosis in rats fed a high-fat diet. J Nutr Biochem 2020;83:108412.

17. Islam KBMS, Fukiya S, Hagio M, Fujii N, Ishizuka S, Ooka T, Ogura Y, Hayashi T, Yokota A. Bile acid is a host factor that regulates the composition of the cecal microbiota in rats. Gastroenterology 2011;141:1773–81.

458 18. Martins PNA, Neuhaus P. Surgical anatomy of the liver, hepatic vasculature and bile ducts
459 in the rat. Liver Int 2007;27:384–92.

460 19. Hori S, Hara H, Ishizuka S. Marginal iron deficiency enhances liver triglyceride
461 accumulation in rats fed a high-sucrose diet. Biosci Biotechnol Biochem 2018;82:2140–8.

462 20. Angelucci E, Brittenham GM, McLaren CE, Ripalti M, Baronciani D, Giardini C,
463 Galimberti M, Polchi P, Lucarelli G. Hepatic iron concentration and total body iron stores in
464 thalassemia major. N Engl J Med 2000;343:327–31.

465 21. Hagio M, Matsumoto M, Ishizuka S. Bile acid analysis in various biological samples
466 using ultra performance liquid chromatography/electrospray ionization-mass spectrometry
467 (UPLC/ESI-MS). Methods Mol Biol 2011;708:119–29.

468 22. Hagio M, Matsumoto M, Fukushima M, Hara H, Ishizuka S. Improved analysis of bile
469 acids in tissues and intestinal contents of rats using LC/ESI-MS. J Lipid Res 2009;50:173–80.

470 23. Lee DG, Hori S, Kohmoto O, Kitta S, Yoshida R, Tanaka Y, Shimizu H, Takahashi K,
471 Nagura T, Uchino H, et al. Ingestion of difructose anhydride III partially suppresses the

472 deconjugation and 7α-dehydroxylation of bile acids in rats fed with a cholic acid-supplemented diet.
473 Biosci Biotechnol Biochem 2019;1–7.

474 24. Chung J, Kim MS, Han SN. Diet-induced obesity leads to decreased hepatic iron storage
475 in mice. Nutr Res 2011;31:915–21.

476 25. Chung H, Wu D, Smith D, Meydani SN, Han SN. Lower hepatic iron storage associated
477 with obesity in mice can be restored by decreasing body fat mass through feeding a low-fat diet.
478 Nutr Res 2016;36:955–63.

479 26. Yamano N, Ikeda Y, Sakama M, Izawa-Ishizawa Y, Kihira Y, Ishizawa K, Miyamoto L,
480 Tomita S, Tsuchiya K, Tamaki T. A long-term high-fat diet changes iron distribution in the body,
481 increasing iron accumulation specifically in the mouse spleen. J Nutr Sci Vitaminol 2015;61:20–7.

482 27. Orr JS, Kennedy A, Anderson-Baucum EK, Webb CD, Fordahl SC, Erikson KM, Zhang
483 Y, Etzerodt A, Moestrup SK, Hasty AH. Obesity alters adipose tissue macrophage iron content and
484 tissue iron distribution. Diabetes 2014;63:421–32.

485 28. Jiang S, Yan K, Sun B, Gao S, Yang X, Ni Y, Ma W, Zhao R. Long-term high-fat diet
486 decreases hepatic iron storage associated with suppressing TFR2 and ZIP14 expression in rats. J
487 Agric Food Chem 2018;66:11612–21.

488 29. Yan Q-W, Yang Q, Mody N, Graham TE, Hsu C-H, Xu Z, Houstis NE, Kahn BB, Rosen
489 ED. The adipokine lipocalin 2 is regulated by obesity and promotes insulin resistance. Diabetes
490 2007;56:2533–40.

491 30. Devireddy LR, Gazin C, Zhu X, Green MR. A cell-surface receptor for lipocalin 24p3
492 selectively mediates apoptosis and iron uptake. Cell 2005;123:1293–305.

493 31. Zhao L, Zhang X, Shen Y, Fang X, Wang Y, Wang F. Obesity and iron deficiency: a
494 quantitative meta-analysis. Obes Rev 2015;16:1081–93.

495 32. Britton L, Bridle K, Reiling J, Santrampurwala N, Wockner L, Ching H, Stuart K,
496 Subramaniam VN, Jeffrey G, St. Pierre T, et al. Hepatic iron concentration correlates with insulin
497 sensitivity in nonalcoholic fatty liver disease. Hepatology Communications 2018;22:778.

33. Siddique A, Nelson JE, Aouizerat B, Yeh MM, Kowdley KV, NASH Clinical Research Network. Iron deficiency in patients with nonalcoholic fatty liver disease is associated with obesity, female gender, and low serum hepcidin. Clin Gastroenterol Hepatol 2014;12:1170–8.

34. Meyerhoffer SM, McGown LB. Critical micelle concentration behavior of sodium taurocholate in water. Langmuir 1990;6:187–91.

35. Xu M-J, Feng D, Wu H, Wang H, Chan Y, Kolls J, Borregaard N, Porse B, Berger T, Mak TW, et al. Liver is the major source of elevated serum lipocalin-2 levels after bacterial infection or partial hepatectomy: A critical role for IL-6/STAT3. Hepatology 2015;61:692–702.

36. Yang J, Goetz D, Li JY, Wang W, Mori K, Setlik D, Du T, Erdjument-Bromage H, Tempst P, Strong R, et al. An iron delivery pathway mediated by a lipocalin. Mol Cell 2002;10:1045–56.

37. Sonnweber T, Ress C, Nairz M, Theurl I, Schroll A, Murphy AT, Wroblewski V, Witcher DR, Moser P, Ebenbichler CF, et al. High-fat diet causes iron deficiency via hepcidin-independent reduction of duodenal iron absorption. J Nutr Biochem 2012;23:1600–8.

38. Bertinato J, Aroche C, Plouffe LJ, Lee M, Murtaza Z, Kenney L, Lavergne C, Aziz A. Diet-induced obese rats have higher iron requirements and are more vulnerable to iron deficiency. Eur J Nutr 2014;53:885–95.

Figure legends

Figure 1

Hepatic concentrations (A) and contents (B) of iron, chromium, manganese, calcium, copper, zinc, and magnesium in WKAH/HkmSlc male rats that were fed either a control or CA diet for 2 weeks (Study 1). *Significantly different from the control ($P < 0.05$). Box and whisker plots show median, minimum, and maximum (n = 8 for the control group and n = 9 for the CA group). CA, cholic acid.

Figure 2

Hepatic iron concentration (A), and iron content (B), hepatic ferritin concentration (C), daily food intake (D), fecal iron excretion (E), aortic plasma iron concentration (F), and ferritin (G), aortic hemoglobin (H), aortic plasma UIBC (I), and TIBC (J), transferrin concentration (K), transferrin saturation (L), hepatic mRNA expression of iron-related genes (M), and aortic plasma LCN2

concentration (N) in WKAH/HkmSlc male rats that were fed either a control or CA diet for 13 weeks (Study 2). In (J), the TIBC was calculated as the sum of the aortic plasma iron concentration (F) and the UIBC (I). In (L), the transferrin saturation was calculated by dividing the aortic plasma iron concentration (F) by the TIBC (J). In (M), the data were normalized to *Rplp0* mRNA expression. *Significantly different from the control ($P < 0.05$). Box and whisker plots show median, minimum, and maximum (n = 12). CA, cholic acid; LCN2, lipocalin 2; *Rplp0*, ribosomal protein lateral stalk subunit P0; TIBC, total iron-binding capacity; UIBC, unsaturated iron-binding capacity.

Figure 3

Aortic plasma total 12αOH BA concentration (A), and total primary 12αOH BA (B), total secondary 12αOH BA (C), TCA (D), CA (E), TDCA (F), DCA (G), hepatic iron concentration (H), and iron content (I), hepatic mRNA expression of LCN2 (J), and aortic plasma LCN2 concentration (K) in male WKAH/HkmSlc rats that were fed either a control or CA diet treated with or without vancomycin (200 mg/L) in drinking water for 6 weeks (Study 3). In (J), the data were normalized to *Rplp0* mRNA expression. Box and whisker plots show median, minimum, and maximum (n = 8).

The *P* values of the Two-way ANOVA (CA and vancomycin) are presented in figures, and further analysis of the simple effect by CA or vancomycin were then performed when there was a significant interaction ($P < 0.05$). *Statistically significant effects of CA diet within the same treatment ($P < 0.0125$). #Statistically significant effects of vancomycin treatment within the same diet ($P < 0.0125$). CA, cholic acid; DCA, deoxycholic acid; 12αOH BA, 12α-hydroxylated bile acid; LCN2, lipocalin 2; *Rplp0*, ribosomal protein lateral stalk subunit P0; TCA, taurocholic acid; TDCA, taurodeoxycholic acid.

Figure 1

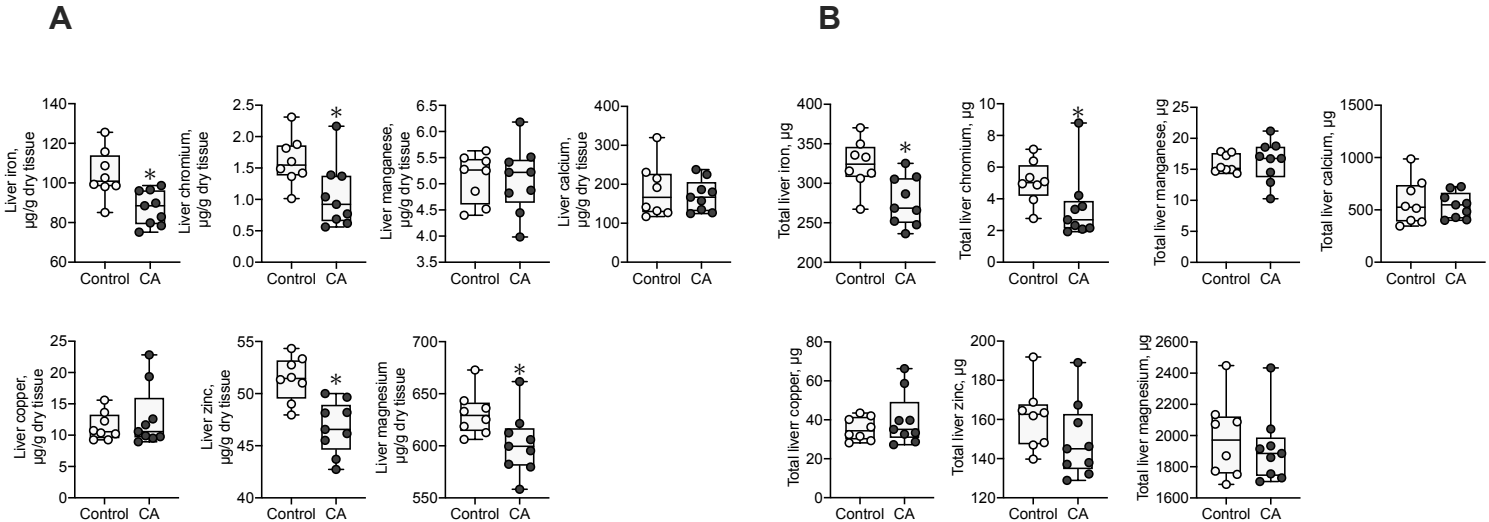
A
B
Liver iron, µg/g dry tissue
Liver chromium, µg/g dry tissue
Liver manganese, µg/g dry tissue
Liver calcium, µg/g dry tissue
Liver copper, µg/g dry tissue
Liver zinc, µg/g dry tissue
Liver magnesium µg/g dry tissue
Total liver iron, µg
Total liver chromium, µg
Total liver manganese, µg
Total liver calcium, µg
Total liverr copper, µg
Total liver zinc, µg
Total liver magnesium, µg
Control
CA
*

Figure 2

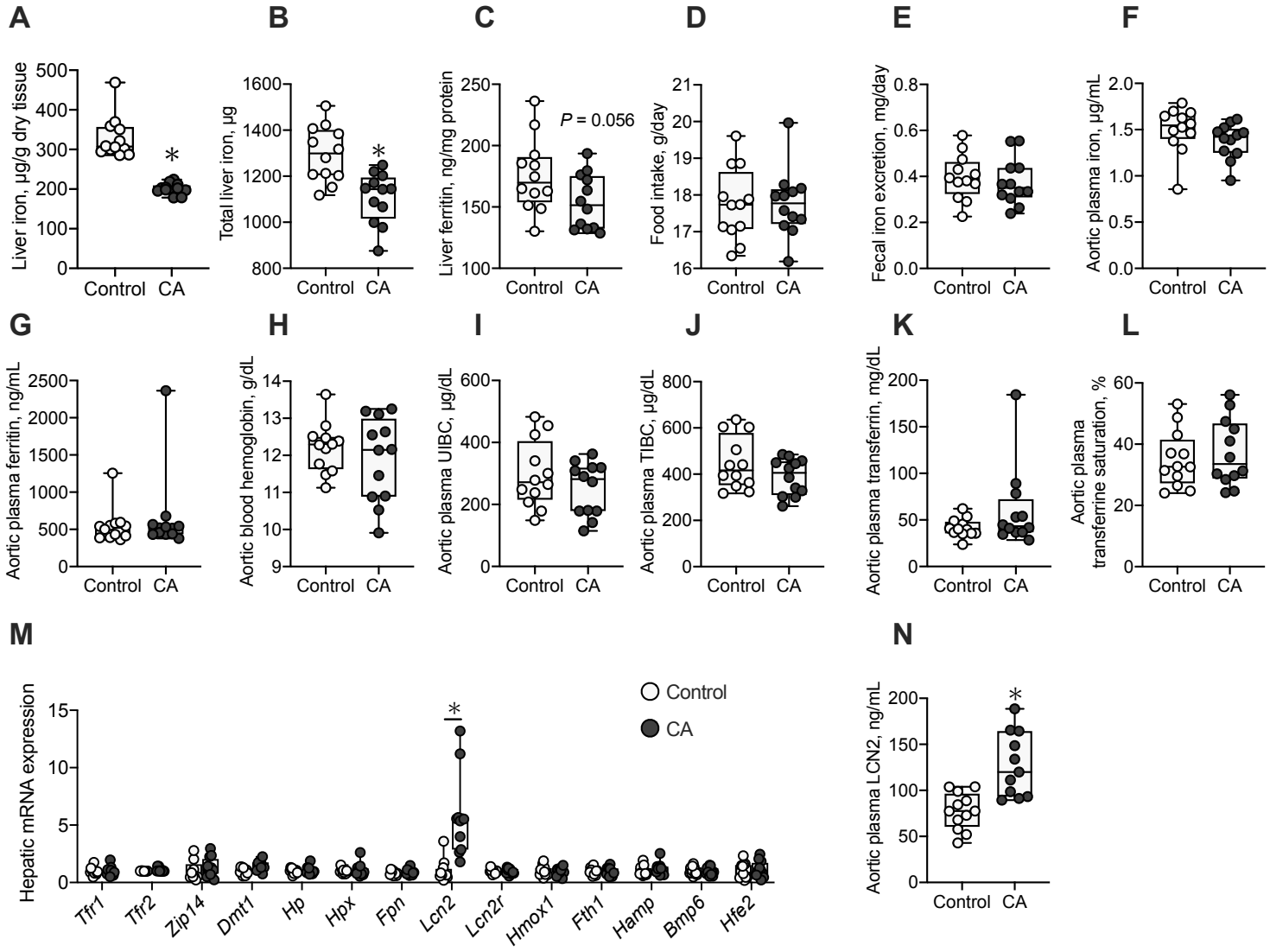
A
Liver iron, µg/g dry tissue
500
400
300
200
100
0
*
Control
CA
B
Total liver iron, µg
1600
1400
1200
1000
800
*
Control
CA
C
Liver ferritin, ng/mg protein
250
200
150
100
P = 0.056
Control
CA
D
Food intake, g/day
21
20
19
18
17
16
Control
CA
E
Fecal iron excretion, mg/day
0.8
0.6
0.4
0.2
0.0
Control
CA
F
Aortic plasma iron, µg/mL
2.0
1.5
1.0
0.5
0.0
Control
CA
G
Aortic plasma ferritin, ng/mL
2500
2000
1500
1000
500
0
Control
CA
H
Aortic blood hemoglobin, g/dL
14
13
12
11
10
9
Control
CA
I
Aortic plasma UIBC, µg/dL
600
400
200
0
Control
CA
J
Aortic plasma TIBC, µg/dL
800
600
400
200
0
Control
CA
K
Aortic plasma transferrin, mg/dL
200
150
100
50
0
Control
CA
L
Aortic plasma transferrine saturation, %
60
40
20
0
Control
CA
M
Hepatic mRNA expression
15
10
5
0
*
Control
CA
Tfr1
Tfr2
Zip14
Dmt1
Hp
Hpx
Fpn
Lcn2
Lcn2r
Hmox1
Fth1
Hamp
Bmp6
Hfe2
N
Aortic plasma LCN2, ng/mL
200
150
100
50
0
*
Control
CA

Figure 3

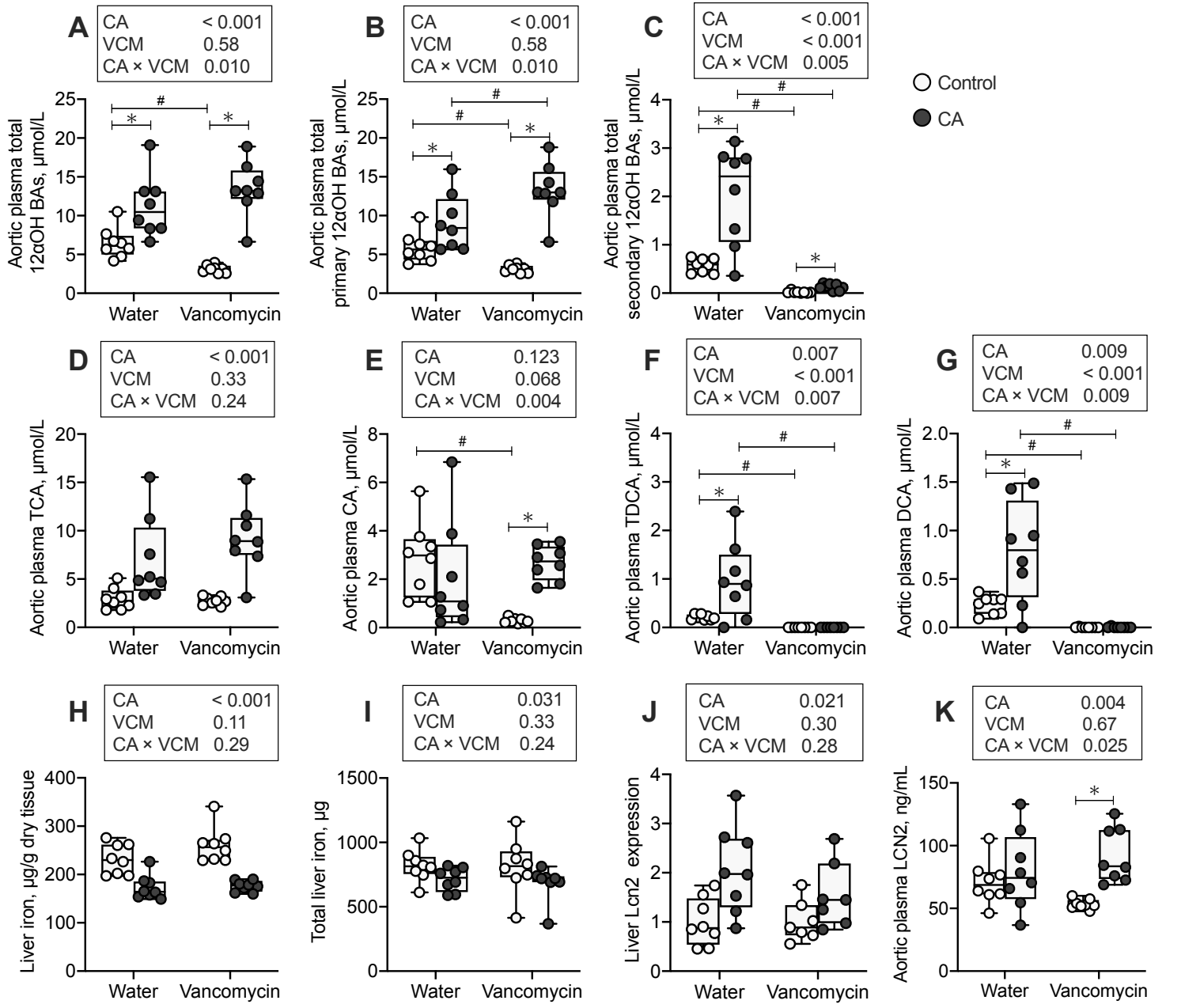
A
CA < 0.001
VCM 0.58
CA × VCM 0.010
Aortic plasma total 12αOH BAs, μmol/L
Water
Vancomycin
B
CA < 0.001
VCM 0.58
CA × VCM 0.010
Aortic plasma total primary 12αOH BAs, μmol/L
C
CA < 0.001
VCM < 0.001
CA × VCM 0.005
Aortic plasma total secondary 12αOH BAs, μmol/L
Control
CA
D
CA < 0.001
VCM 0.33
CA × VCM 0.24
Aortic plasma TCA, μmol/L
E
CA 0.123
VCM 0.068
CA × VCM 0.004
Aortic plasma CA, μmol/L
F
CA 0.007
VCM < 0.001
CA × VCM 0.007
Aortic plasma TDCA, μmol/L
G
CA 0.009
VCM < 0.001
CA × VCM 0.009
Aortic plasma DCA, μmol/L
H
CA < 0.001
VCM 0.11
CA × VCM 0.29
Liver iron, μg/g dry tissue
I
CA 0.031
VCM 0.33
CA × VCM 0.24
Total liver iron, μg
J
CA 0.021
VCM 0.30
CA × VCM 0.28
Liver Lcn2 expression
K
CA 0.004
VCM 0.67
CA × VCM 0.025
Aortic plasma LCN2, ng/mL